J. Electrochem. Sci. Eng. **15(4)** (2025) 2615; http://dx.doi.org/10.5599/jese.2615

Open Access : : ISSN 1847-9286
www.jESE-online.org

Original scientific paper

Pitting corrosion characteristics of gas tungsten arc welded austenitic steel

Abraham M. Afabor[1,✉], Basil O. Onyekpe[2], Oghenerobo Awheme[2] and Cyril O. Uyeri[1]

[1]*Delta State University of Science and Technology, Ozoro, Nigeria*
[2]*University of Benin, Benin City Edo State Nigeria*

Corresponding author: ✉*afabormartins2@gmail.com*

Received: October 24, 2024; Accepted: June 2, 2025; Published: June 6, 2025

Abstract

This study utilized a hybrid optimization technique, specifically the Taguchi-based grey-fuzzy logic, to optimize gas tungsten arc welding parameters with regard to tensile strength and hardness of 316L austenitic stainless steel. The Taguchi L27 orthogonal design of experiments was employed to optimize four input parameters: welding current, speed, voltage, and gas flow rate, to assess the pitting corrosion properties of the steel. Potentiodynamic polarization tests using a potentiostat were conducted to evaluate the pitting corrosion resistance of the welded samples. Microstructural analyses, aided by scanning electron microscopy, were performed to assess the surface morphologies of the steel samples. Subsequently, a confirmatory experiment was carried out to validate the optimization technique used. The results obtained indicate that the optimal welding parameters are a current of 95 A, speed of 0.7 mm/s, voltage of 25 V, and gas flow rate of 20 L/min, showing that the optimized steel sample exhibited an improvement in the multi-response performance index in terms of mechanical properties from 0.0409 to 0.495. By utilizing the strengths of both methods and integrating this hybrid optimization technique, the study provides valuable insights into the relationship between welding parameters and corrosion resistance, ultimately contributing to the development of more durable and reliable stainless-steel components.

Keywords

Stainless steel; welding parameters; hybrid optimization; potentiodynamic polarization; localized corrosion

Introduction

Welds in austenitic stainless steels are associated with two significant issues: hot cracking of the weld metal and sensitization of the weld heat-affected zone. Localized corrosion occurs in the heat-affected region as a result of sensitization. Chromium carbide precipitation and formation at grain boundaries in the heat-affected zone are the causes of sensitization when heated within the 427 to

871 °C temperature range. However, the material cools at a slower rate, and to reduce the duration in this sensitization temperature range, the base material must not be preheated, and welding should be conducted with the lowest possible heat input that still results in a high-quality weld. The corrosion resistance of these local areas is reduced as a result of the removal of some chromium from solution near the grain boundaries by chromium carbide formation, as the majority of carbon is located near grain boundaries. This issue can be resolved by employing low-carbon base and filler materials to decrease the quantity of carbon available for chromium to combine.

The degree of carbide precipitation increases with higher carbon content and the time spent at the critical mid-range temperatures. Welding naturally produces a temperature gradient in the steel. It ranges from the melting temperature at the weld to room temperature, some distance from the weld. For an adequate period, a limited zone on either side of the weld remains within the sensitizing temperature range, allowing precipitation to occur. When employed in exceedingly corrosive environments, each weld develops detrimental corrosion lines. The quantity of carbide precipitation is reduced by fostering rapid cooling. Another factor in preventing carbide precipitation is the use of the appropriate type and quantity of shielding gas. Pure argon typically yields the most favorable outcomes when welding thin austenitic stainless steel. However, a small quantity of hydrogen is not uncommon when a faster travel speed is required, particularly for thicker pieces or an automated application. Annealing the weldment at 1038 °C or higher, followed by water quench, a post-weld heat treatment procedure, eliminates carbide precipitation, but this is an expensive and often impractical procedure.

The problem of carbide precipitation arising from sensitization could be avoided by reducing sulphur and phosphorus to very low amounts, but this would significantly increase the cost of making the steel. Austenitic stainless steel can be susceptible to sensitization, which occurs when chromium carbides form at grain boundaries due to improper welding parameters or exposure to high temperatures. Sensitized stainless steel becomes susceptible to pitting and intergranular corrosion, leading to a degradation of the material's corrosion resistance. By optimizing welding parameters, the risk of sensitization can be minimized, preserving the stainless steel's corrosion resistance.

Austenitic stainless steel is commonly used in applications with critical corrosion resistance and mechanical properties. By optimizing welding parameters, high-quality welds with good fusion, minimal defects (such as porosity, cracks, or inclusions), and limited distortion can be achieved. This ensures the integrity of the welded structure and helps to maintain the desired properties of the stainless steel.

The grey integrated with Taguchi-fuzzy logic approach as applied by [1] was used in the study of parametric influence and welding performance optimization during regulated metal deposition.

Taguchi-based fuzzy logic was successfully utilized in optimizing tungsten inert gas (TIG) welding parameters on the dilution and hardness of AA5052 aluminum alloy [2]. Pondi *et al.* [3] predicted the optimization of tungsten inert gas welding process parameters using design of experiments together with fuzzy logic. Sridevi *et al.* [4] investigated the process parameter optimization during EDM of AISI 316 LN stainless steel by using fuzzy-based multi-objective PSO. Ankit *et al.* [5] used a hybrid RSM-based grey-fuzzy technique in the multi-objective optimization of electric discharge machining process parameters. Vijayan and Seshagiri [6] did an investigation of the optimization of friction stir welding process parameters using the RSM-based grey–fuzzy approach. Winarni and Sapto [7] undertook a study of the application of multi-response optimization of electrical discharge machining using grey relational analysis and the fuzzy logic method. Moganapriya *et al*. [8] worked

on obtaining machining effectiveness for AISI 1015 structural steel through coated inserts using the Taguchi method, grey relational analysis, and fuzzy logic.

Optimal selection and precise control of welding process parameters can achieve very satisfactory weld quality devoid of the aforementioned defects in terms of mechanical properties and corrosion resistance. Optimizing welding parameters for austenitic stainless steel is crucial to achieving high-quality welds, preserving corrosion resistance, maximizing productivity, and ensuring structural integrity. It requires careful consideration of parameters like travel speed, heat input, electrode selection, shielding gas, preheating, and interpass temperatures to achieve the desired weld characteristics and properties. Hence, an integrated Taguchi-based grey-fuzzy optimization technique has been proposed for the optimization of gas tungsten arc welding (GTAW) parameters and their effect on the mechanical properties of AISI 316L austenitic stainless steel. The welding parameters selected to be optimized in this study were those adopted from [9], though with an additional welding parameter of speed included and a hybrid multi-objective optimization employed. These parameter ranges were chosen to align with common industrial practices and experimental feasibility. These ranges reflect practical conditions in welding operations and align with prior studies [3,9] demonstrating effective heat input and weld quality control. The choice of the integrated Taguchi-based grey-fuzzy optimization technique is predicated on the ability of the Taguchi method to provide a robust design of experiments framework, while grey-fuzzy logic enables the handling of uncertainty, ambiguity and the ability to model complex relationships between welding variables in the optimization process.

Experimental

Test material and sample preparation

The test material used in this study was commercial AISI 316L austenitic stainless steel with a thickness of 10 mm; the GTAW parameters are as presented in [9]. As determined by X-ray diffraction, the elemental chemical composition of the base metal and filler metal is as displayed in [9].

Four parameters were chosen for this study, including gas flow rate, current, speed, and voltage for the optimization of the welding process. These parameters were chosen based on literature reviews and industrial expertise to ensure relevance and accuracy. A down-hand flat position was used during the welding process. Single V-butt joints with an included bevel angle of 60° between AISI 316L steel with a root gap of 2 mm, as shown in [9], were welded by GTA welding using ER 316L filler metal wire. Selected input parameters were employed to fabricate V-butt joints. ASTM-standard tensile test samples with their weld bead located at the centre of each sample were prepared. The welding set-up was as described in [9]. Experimental tensile test samples used for this study are shown in Figure 1.

Figure 1. *Experimental steel samples*

Optimization method

Taguchi design of experiment

The GTAW parameters and their levels are presented in Table 1. The Taguchi design of experiments was used for carrying out all the experiments, by which the Taguchi L27 orthogonal array with 3 levels of 4 factors was used, as shown in Table 2, presented with results below. Welding is a complex process, and interactions between its parameters play a significant role; therefore, for high precision and reliability of the optimization process, the Taguchi L27 orthogonal array of design of experiments was adopted for this study.

Table 1. *GTA welding parameters and their levels*

Parameter	Code	Level 1 (low)	Level 2 (medium)	Level 3 (high)
Current, A	J	95	100	105
Speed, mm s^{-1}	K	0.7	0.9	1.1
Voltage, V	L	23	25	27
Gas flow rate, L min^{-1}	M	10	15	20

Table 2*. Experimental results based on Taguchi L27 design of experiment*

Exp. No.	J	K	L	M	Signal-noise-ratio (SNR) 1 (dB)	Normalized value of tensile strength	Signal-noise-ratio (SNR) 2 (dB)	Normalized value of microhardness
1	J_1	K_1	L_1	M_1	55.0410	0.000	44.9004	0.0218
2	J_1	K_1	L_1	M_1	55.1373	0.076	44.8359	0.0000
3	J_1	K_1	L_1	M_1	55.1843	0.113	45.1055	0.0913
4	J_1	K_2	L_2	M_2	55.3846	0.271	45.7471	0.3084
5	J_1	K_2	L_2	M_2	55.3119	0.214	45.8628	0.3476
6	J_1	K_2	L_2	M_2	55.4244	0.302	45.6886	0.2886
7	J_1	K_3	L_3	M_3	55.5093	0.369	46.8603	0.6852
8	J_1	K_3	L_3	M_3	55.4787	0.345	46.9271	0.7078
9	J_1	K_3	L_3	M_3	55.4435	0.317	46.9778	0.7250
10	J_2	K_1	L_2	M_3	56.2181	0.928	47.7904	1.0000
11	J_2	K_1	L_2	M_3	56.3089	1.000	47.6942	0.9674
12	J_2	K_1	L_2	M_3	56.1737	0.8934	47.7620	0.9904
13	J_2	K_2	L_3	M_1	56.0746	0.8152	46.8049	0.6664
14	J_2	K_2	L_3	M_1	55.9190	0.6925	46.8800	0.6919
15	J_2	K_2	L_3	M_1	55.9951	0.7525	46.7651	0.6530
16	J_2	K_3	L_1	M_2	55.6322	0.4662	46.8916	0.6958
17	J_2	K_3	L_1	M_2	55.5558	0.4060	46.8326	0.6758
18	J_2	K_3	L_1	M_2	55.5630	0.4117	46.9310	0.7091
19	J_3	K_1	L_3	M_2	55.4273	0.3047	46.4733	0.5542
20	J_3	K_1	L_3	M_2	55.5963	0.4380	46.5594	0.5833
21	J_3	K_1	L_3	M_2	55.6437	0.4754	46.4278	0.5388
22	J_3	K_2	L_1	M_3	55.5383	0.3922	46.8287	0.6745
23	J_3	K_2	L_1	M_3	55.4816	0.3475	46.8089	0.6678
24	J_3	K_2	L_1	M_3	55.4111	0.2919	46.8760	0.6905
25	J_3	K_3	L_2	M_1	55.4185	0.2977	46.7532	0.6489
26	J_3	K_3	L_2	M_1	55.3119	0.2137	46.7771	0.6570
27	J_3	K_3	L_2	M_1	55.5659	0.4140	46.8128	0.6691

Grey-fuzzy optimization analysis

Designing a grey-fuzzy optimization technique involves the following steps [7]:

1. Plan the experiments accordingly, with the appropriate Taguchi orthogonal array determining the level of welding parameters.
2. Normalize the experimental results of mechanical properties—in this study, tensile strength and microhardness—according to the procedure of grey relational analysis.

3. Calculate the grey relational coefficient and grey relation grade for the mechanical property response.
4. Establish the triangular membership function and fuzzy rule to fuzzify the grey relational coefficient of each response.
5. Use the maximum-minimum interface operation to calculate the fuzzy output, and convert the result into a grey-fuzzy-grade (GFG).
6. Use the response table and graph to determine the ideal welding parameter settings.
7. Confirm the test and verify the optimal setting of welding parameters.

Signal-to-noise ratios

The tensile strength and microhardness are larger-the-better performance characteristics since the maximization of the quality characteristic of interest is sought and can be expressed as Equation (1) [7]:

$$\text{SNR} = -10 \log\left(\sum_{i=1}^{n} \frac{y_i^{-2}}{n}\right) \quad (1)$$

where n = number of replications, y = observed value, and i = 1, 2 …, n,

Normalizing signal-to-noise ratios

Higher values for microhardness and tensile strength are desired. Hence, 'higher the better' normalization criteria are considered for microhardness and tensile strength. The formula for the 'higher-the-better' normalization criteria considered is as presented in Equation (2) [10,11]:

$$x_j(n) = \frac{y_j(n) - y_{j(\text{min.})}}{y_{j(\text{max.})} - y_{j(\text{min.})}} \quad (2)$$

$x_i(n)$ = normalized grey relational value, $y_i(n)$ = SNR for the n^{th} response, $y_{j(\text{min})}$ = lowest value of $y_j(n)$ for the n^{th} response, $y_{j(\text{max})}$ = highest value of the $y_j(n)$ for the n^{th} response.

Grey relational coefficients

The grey relational coefficient (GRC) of each target value and reference value on the corresponding elements is calculated, respectively. The GRCs on the normalized SNR values can be calculated as per Equation (3) [6]. The obtained results are presented in Table 2.

$$\Gamma_j(n) = \frac{\Delta_{\text{min.}} + \xi\Delta_{\text{max.}}}{\Delta_j(n) + \xi\Delta_{\text{max.}}} \quad (3)$$

Where $\Gamma_j(n)$ = grey relational coefficient, $\Delta_j(n) = |x_0 - x_i(n)|$ is the absolute value of the difference between the target value and the reference value; $\Delta_{\text{min.}}$= absolute value of the minimum difference between the target value and the reference value; $\Delta_{\text{max.}}$= absolute value of the maximum difference between the target value and the reference value, ξ = 0.5 is the resolution coefficient (between 0 and 1), usually takes a value of 0.5. This is so because it allows for a more balanced comparison between different alternatives, as it is less sensitive to extreme values or outliers in the data. The smaller the value of ξ, the greater the difference between correlation coefficients, and the stronger the discrimination ability becomes.

Grey relation grade

The grey relation grade is calculated as per Equation (4) [8]:

$$\gamma_j(n) = \frac{1}{m}\sum_{n=1}^{m} \Gamma_j(n) \quad (4)$$

When each response data has different weights in the comprehensive evaluation, it is necessary to consider the weight coefficient of the response to get the weighted average (W_n) value in solving the GRG as per Equation (5) [6]:

$$\gamma_j(n) = \frac{1}{m}\sum_{n=1}^{m} \mathrm{W}_n \ \Gamma_j(n), \ \sum_{n=1}^{m} W_n = 1 \quad n = 1,2, \ldots m \tag{5}$$

where W_n is the given weight to the n^{th} factor, and m is the number of response characteristics.

The weightages were given as 0.6 and 0.4 for the grey relational coefficient of tensile strength and the grey relational coefficient of microhardness, respectively.

Finally, the correlation degree (or GRG) between the target value and the reference value is sorted from large to small (*i.e.* ranked), as displayed in Table 3, and the larger the correlation degree, the more consistent is the change situation between the target value and the reference value.

Table 3. *Computed GRG and GFG values*

Exp. No.	GRC		GRG	GRG rank	GFG	GFG rank
	Ultimate tensile strength	Hardness				
1	0.333	0.338	0.1675	27	0.0801	27
2	0.351	0.333	0.1719	26	0.0806	26
3	0.360	0.355	0.1790	25	0.0810	25
4	0.407	0.420	0.2061	23	0.1506	23
5	0.389	0.434	0.2035	24	0.1502	24
6	0.417	0.413	0.2077	22	0.164	22
7	0.442	0.614	0.2554	14	0.3060	14
8	0.433	0.631	0.2561	12	0.2960	16
9	0.423	0.645	0.2559	13	0.2820	`17
10	0.874	1.000	0.4622	2	0.8160	2
11	1.000	0.939	0.4878	1	0.9160	1
12	0.824	0.981	0.4434	3	0.7700	3
13	0.730	0.600	0.3390	4	0.5000	5
14	0.619	0.619	0.3095	6	0.5000	5
15	0.669	0.590	0.3187	5	0.4860	6
16	0.484	0.622	0.2696	7	0.3560	7
17	0.457	0.607	0.2585	9	0.3240	12
18	0.459	0.632	0.2641	8	0.3280	11
19	0.418	0.529	0.2312	21	0.2680	20
20	0.471	0.545	0.2503	17	0.3340	9
21	0.488	0.520	0.2504	16	0.3440	8
22	0.451	0.606	0.2565	11	0.3180	13
23	0.434	0.601	0.2504	16	0.2960	16
24	0.414	0.618	0.2478	18	0.2700	19
25	0.416	0.587	0.2422	19	0.2720	18
26	0.389	0.593	0.2353	20	0.2500	21
27	0.460	0.602	0.2584	10	0.3280	11

Fuzzy-grey relational grade

Fuzzy logic GRG analysis is divided into fuzzifier, fuzzy engine inference, and defuzzifier. Using MATLAB, with fuzzy sets of input, output variables can be formed using fuzzy rules presented in Figure 2. Based on the above discussion, the larger the multi-response performance index (MRPI), the better the performance characteristic.

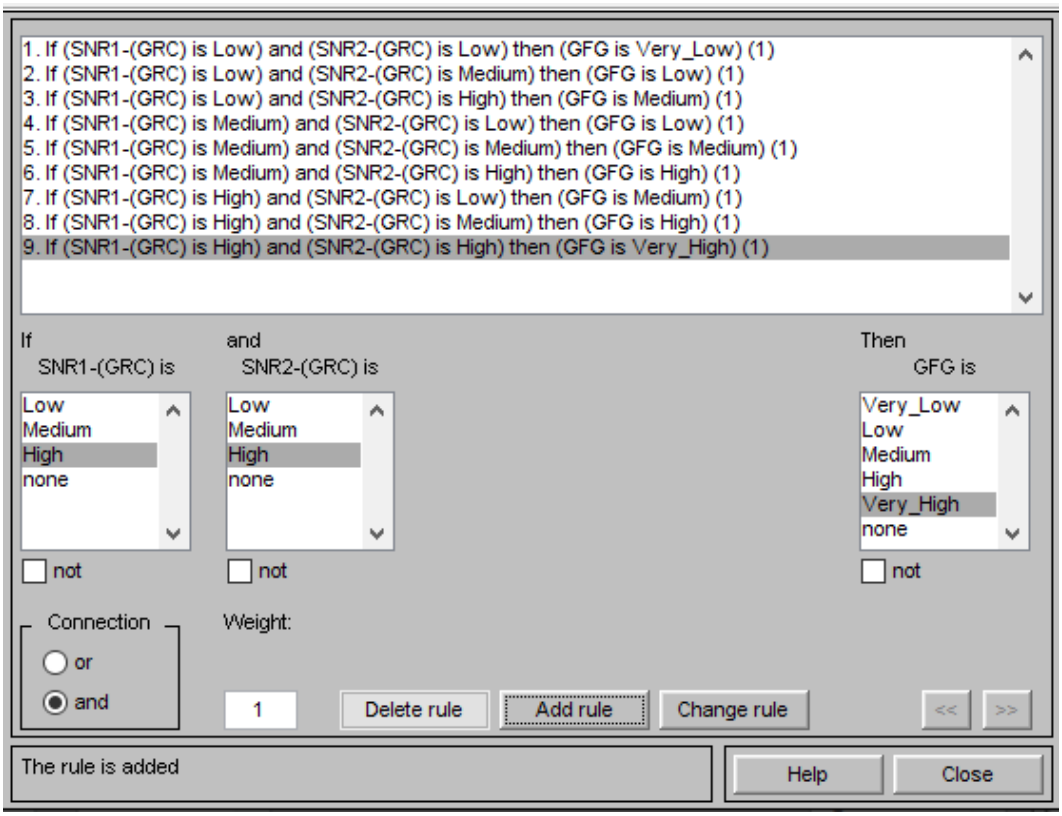

Figure 2. *Fuzzy subsets of input and output variables generated from MATLAB software*

Microstructural examination

Three samples (base metal, non-optimized, and optimized steel samples) were polished and etched with Nital, after which they were examined using the Carl Zeiss Smart Evo 10 Scanning Electron Microscope.

Pitting corrosion test procedure

The analysis was carried out on a Metrohm Autolab PG Stat 202 Potentiostat. A 3-electrode cell setup was created using the specimen as the working electrode, a stainless-steel counter electrode, and a silver/silver chloride (Ag/AgCl) reference electrode. Before starting, a base potential is established. Following the stabilization of the corrosion potential (E_{corr}), the applied potential is increased at a gradual pace in the positive direction compared to the reference electrode. The potentiodynamic polarization (PDP) experiment was carried out within a potential window ranging between -0.5 and 0.45 V *vs.* Ag/AgCl at a scan rate of 20 mV s^{-1}. The corrosion rate was automatically evaluated using the AutoLab Nova 2.1 software, employing the polarization resistance method. The corrosion characteristics are predicted from the polarization scan produced by a potentiostat. This technique aims to set up a potentiodynamic polarization corrosion system to analyse the pitting corrosion of the steel samples in a seawater environment with composition given in Table 4.

Table 4. *Composition of the seawater used for PDP experiments*

Content of dissolved oxygen at 27.5 °C, mg l^{-1}	8.20
pH at 27.5 °C	7.45
Sodium content, mg l^{-1}	6.84
Salinity in form of chloride, mg l^{-1}	7010.7
Sulphate content, mg l^{-1}	6.96

Results and discussion

Using the Taguchi L27 orthogonal array (OA) technique, the designed experimental layout yielded the following response values of micro-hardness and tensile strength. In this study, tensile strength and micro hardness are considered to be the quality characteristics of the welding process. The experimental test results, the calculated signal-to-noise ratios (SNR), and normalized values are presented in Table 2.

The effects of the grey relational coefficient on the grey fuzzy reasoning grade are displayed in Table 3, which shows the summary of GRGs and their corresponding ranks. From Table 3, experiment No. 11 has the highest value of both the grey relational grade (GRG) and the grey fuzzy grades (GFG), and hence it was allotted as rank one. The optimal setting of the process parameter is to achieve a higher grey fuzzy relational grade. Since the optimal setting of process parameters represents the relationship between the reference sequence and objective sequence, a greater fuzzy grey relational grade reveals that the objective sequence has a stronger relationship than the reference sequence.

Confirmatory test

A confirmatory experiment was conducted utilizing the optimal levels of the GTA welding parameters derived from the Taguchi-fuzzy logic technique and Equation (6) [12,13]. The GFG was calculated or predicted to verify and validate the enhancement of the multiple response performance index. Table 5 presents the predicted and actual GFG values, increasing from 0.0409 to 0.495. Consequently, based on the results of the confirmatory experiment, the optimal combination of welding parameters was determined to be a welding current of 100 A, a speed of 0.7 mm s^{-1}, a voltage of 25 V, and a gas flow rate of 20 L min^{-1} ($J_2K_1L_2M_3$).

$$\mathrm{N} = \mathrm{N_a} + \sum_{j=1}^{n} \left(N_\mathrm{r} - \mathrm{N_a} \right) \tag{6}$$

where N is the calculated or predicted GFG, $N_a$is the average or mean of the total of the GFGs of all the runs, N_r is the average of the GFGs at the required level of the process parameters, and n is the relevant welding process parameter of the GFG.

The experimental validation yielded a maximum SNR 1 of 56.3556 and a maximum SNR 2 of 47.7407, both achieved by the optimized steel sample, as presented in Table 5.

Table 5. *Validation test results*

Level combination	Initial levels of welding parameters	Optimal levels of welding parameters	
	Experiment	Prediction	Experiment
	$J_1K_1L_1M_1$	$J_2K_1L_2M_3$	$J_2K_1L_2M_3$
SNR 1	55.1661		56.3553
SNR 2	45.2822		47.7407
GFG	0.0409	0.417	0.495
Improvement in GFG reasoning		0.4541	

Morphological performance

Figures 3a to 3c present the SEM micrographs of the optimized, non-optimized, and base metal steel samples, respectively. The fine-grain structure of the optimized steel sample, as shown in the SEM in Figure 3a, contributes to its superior multiple performance response compared to the coarse-grain structure of the non-optimized steel sample depicted in Figure 3b, which accounts for its lower performance response.

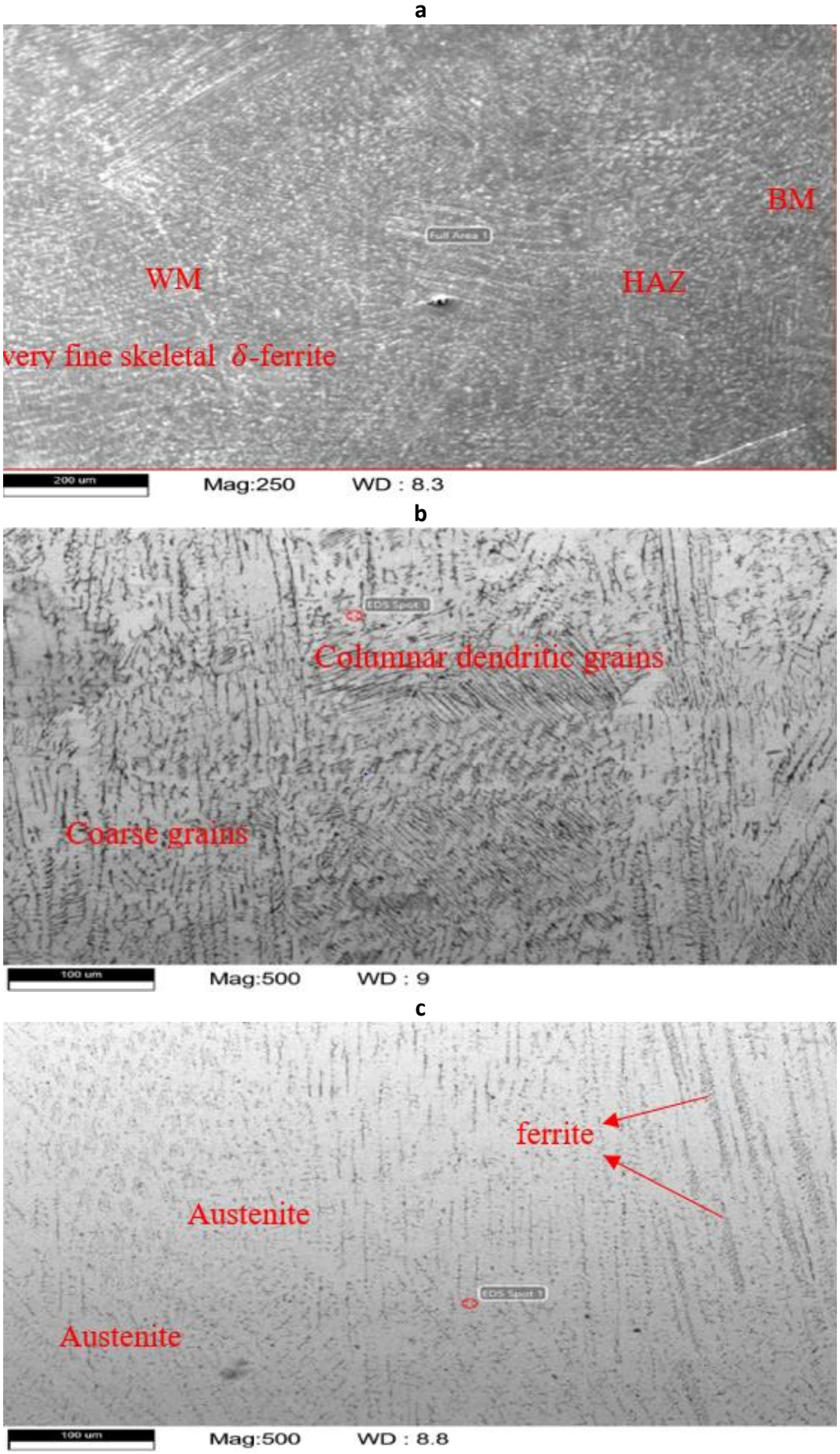

Figure 3. *SEM micrograph of a - optimized steel sample; b- non-optimized steel sample and c - base metal*

Pitting corrosion performance and evaluation

The potentiodynamic polarization plots for the steel samples used for the confirmatory test, which include the non-optimized steel sample, optimized steel sample, and control sample (base metal) in sea-water environment (Table 4), are presented in Figures 4 to 6.

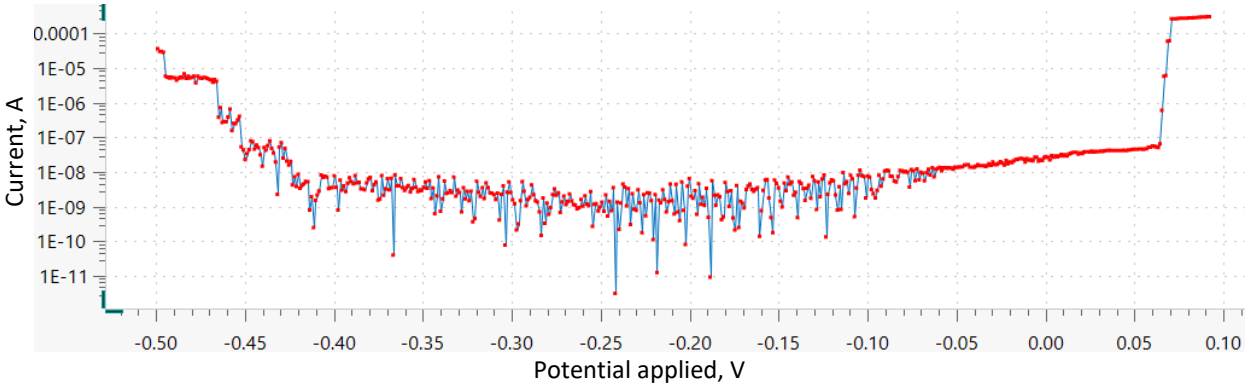

Figure 4. *Potentiodynamic polarization plot for the non-optimized steel sample*

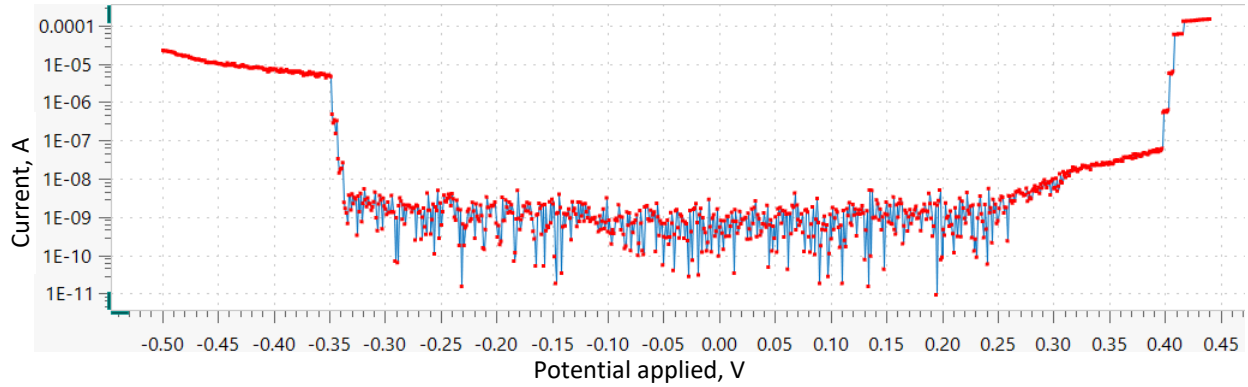

Figure 5. *Potentiodynamic polarization plot for the optimized steel sample*

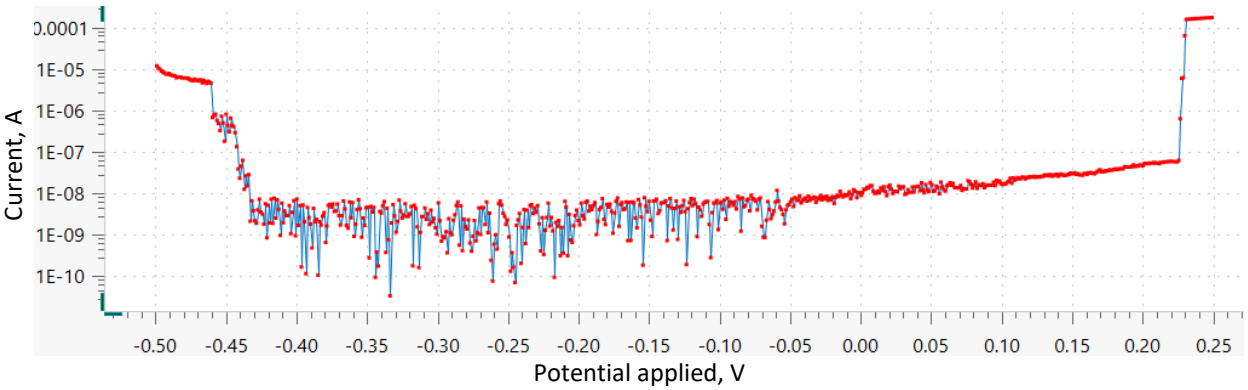

Figure 6. *Potentiodynamic polarization plot for the base metal*

From the potentiodynamic polarization plots, the values of the parameters E_{corr}, I_{corr}, R_p, and corrosion rate were determined as given in Table 6.

Table 6*. Results of potentiodynamic polarization measurements*

Sample	E_{corr} / V	j_{corr} / µA cm^{-2}	i_{corr} / µA	Corrosion rate, mm year^{-1}	R_p / Ω
Non-optimized	-0.43	0.111	0.0392	0.0013	664685.70
Optimized	-0.33	10.9	0.0338	0.1300	7686.90
Base metal	-0.44	18.2	5.3300	0.2120	4888.65

The potentiodynamic measurements provide an assessment of corrosion behavior under static conditions. The measurements are instantaneous and provide rapid measurement of reactions involving rapid electron transfer. The goal was to determine the pitting corrosion resistance of 316L austenitic stainless steel in a seawater environment.

The PDP curves clearly show the active-passive transition stage highlighted by an initial increase in current followed by a sharp decrease, indicating a transition from active to passive behavior. The passive region in the curves is illustrated by a low current plateau, passivation current, indicating the formation of a protective oxide layer of Cr_2O_3. The pitting potential (E_{pit}) occurs at the point of sudden increase in current, indicating breakdown of the passive layer and initiation of pitting corrosion. The PDP results from the confirmatory test indicate that the base metal has a significantly higher corrosion rate compared to the non-optimized and optimized welded samples. This suggests that the control sample (base metal) has greater susceptibility to general corrosion than the optimized sample with a polarization resistance value of 4888.65 Ω, followed by the non-optimized steel sample with the least susceptibility to general corrosion, and this is exemplified by its low corrosion rate. The SEM of the base metal, as displayed in Figure 3c, reveals a fine, equiaxed grain structure with a greater grain boundary area than the welded samples. The low corrosion susceptibility of the non-optimized steel sample could be attributed to the filler metal used for the welding, having a higher amount of chromium than the base metal, possibly implying that the influence of alloying metals on corrosion resistance is higher than that of grain boundaries. The non-optimized steel sample with a polarization resistance of 664685.7 Ω exhibited a significantly higher resistance to corrosion than the other samples under evaluation, with the least corrosion rate of 0.0013 mm $year^{-1}$. In contrast to static immersion testing, the potentiodynamic polarization measurements in dynamic conditions (solution agitation) may accelerate corrosion. Therefore, it is expected that the potentiodynamic corrosion rates observed in the aqueous test solution, which range from 0.001 to 0.2 mm $year^{-1}$, are anticipated to be substantially lower than the rates for the dynamic immersion experiments conducted at room temperature.

The PDP plots displayed in Figures 4 to 6 reveal that the optimized steel sample exhibited the highest pitting potential with an E_{pit} value of 0.40 V, followed by the base metal with an E_{pit} value of 0.22 V, and the non-optimized steel sample exhibited the least pitting potential with an E_{pit} value of 0.06 V. The optimized steel sample also displayed a wider passive region with a range of (-0.34 to 0.4 V), then the base metal with a passive region range of (-0.43 to 0.22 V), and next, the non-optimized steel sample with the narrowest passive region range of (-0.40 to 0.06 V). All the samples exhibited similar passivation current values. It can be concluded that the optimized steel sample shows improved protection against pitting corrosion as an indicator of superior passivation behavior and increased resistance to localized corrosion, while the non-optimized steel sample shows the lowest susceptibility to pitting corrosion.

Conclusion

The influence of GTA welding input parameters on the weldment functionality is investigated. Based on the experimental results and their interpretation, discussion, modeling, and analyses, the findings from this study are as follows:

1. The optimal parametric settings for gas tungsten arc welding of 316L austenitic stainless steel using a Taguchi-based grey-fuzzy logic hybrid optimization technique were current of 95 A, speed at 0.7 mm s^{-1}, voltage of 25 V, and gas flow rate of 20 L min^{-1}.

2. The percentage error between the predicted results (GFG = 0.417) and the results of the confirmatory test (GFG = 0.495) is found to be less than 19 %, which validates the proposed optimization procedure.
3. The optimized steel sample exhibited the least susceptibility to pitting corrosion resistance with a passive region range of (-0.34 to 0.4 V), followed by the base metal (-0.43 to 0.22 V), and the non-optimized steel sample -0.40 to 0.06 V), respectively.

By utilizing the strength of both methods and integrating this hybrid optimization technique, the study provides valuable insights into the inter-relationship between welding parameters and mechanical properties, ultimately contributing to the development of more durable and reliable stainless-steel components. The research highlights the potential benefits of using hybrid optimization techniques in materials processing and welding applications, paving the way for future studies and industrial applications, which include advanced welding processes, new materials, and complex corrosion environments.

***Acknowledgements**: This research was funded by TETFUND Nigeria in collaboration with Southern Delta University (Formerly Delta State University of Science and Technology Ozoro, Nigeria).*

***Conflict of interest**: The authors declare no conflict of interest.*

References

[1] P. Vishalkumar, J. J. Vora, S. Das, K. Abhishek, Study of parametric influence and welding performance optimization during regulated metal deposition (RMD) using grey integrated with fuzzy Taguchi approach, *Journal of Manufacturing Processes* **54** (2020) 286-300. http://dx.doi.org/10.1016/j.jmapro.2020.03.017

[2] S. Omprakasam, R. Raghu, C. B. Ayyanar, Multi-objective welding optimization for AA5052 using Taguchi-fuzzy approach*, SAE International Journal of Materials and Manufacturing* **18(3)** (2025). https://doi.org/10.4271/05-18-03-0018

[3] P. Pondi, J. Achebo, A. Ozigagun, Prediction of tungsten inert gas welding process parameters using design of experiment and fuzzy logic, *Journal of Advances in Science and* Engineering **4** (2021) 86-97. https://doi.org/10.37121/jase.v4i2.149

[4] G. Sridevi, K. C. Rath, S. Mishra, S. Patro, P. S. Rao, *Optimization of EDM Process Parameters with Fuzzy Logic Technique for SS-316 Steel and Investigation of Microstructural Characteristics of EDM Machining Surface,* in: *Evolutionary Manufacturing, Design and Operational Practices for Resource and Environmental Sustainability*, K. Muduli, S. Kumar Rout, S. Sarangi, S.M.N. Islam, A. Mohamed (Eds.), Scrivener Publ. LLC, 2024, pp. 245-256. https://doi.org/10.1002/9781394198221.ch21

[5] S. Ankit, V. Kumar, A. Babbar, V. Dhawan, K. Kotecha, C. Prakash, Experimental investigation and optimization of electric discharge machining process parameters using grey-fuzzy-based hybrid techniques, *Materials* **14(19)** (2021) 5820. https://doi.org/10.3390/ma14195820

[6] D. Vijayan, R.V. Seshagiri. Optimization of friction stir welding process parameters using RSM-based Grey–Fuzzy approach, *Saudi Journal of Engineering and Technology* **2(1)** (2017) 12-25. https://saudijournals.com/articles/2584/

[7] S. Winarni, W. I. Sapto, Application of multi-response optimization with grey relational analysis and fuzzy logic method, *IOP Conference series: Journal of Physics: Conference Series* **948** (2018) 012075. https://doi.org/10.1088/1742-6596/948/1/012075

[8] C. Moganapriya, R. Rajasekar, P.S. Kumar, T. Mohanraj, V. K. Gobinath, J. Saravanakumar, Achieving machining effectiveness for AISI 1015 structural steel through coated inserts and grey-fuzzy coupled Taguchi optimization approach, *Structural and Multidisciplinary Optimization,* **63** (2021) 1169-1186. https://doi.org/10.1007/s00158-020-02751-9

[9] A. M. Afabor, D. F. Ikikiru, Parametric optimization of gas tungsten arc welding (GTAW) on the tensile strength of AISI 316L austenitic stainless steel using Taguchi method, *Journal of Materials Engineering, Structures and Computation,* **1** (1) (2022) 90-101. https://doi.org/10.5281/zenodo.7525254

[10] S. Karumuri, B. Haldar, A. Pradeep, S. A. K. Karanam, M. N. S. Sri, P. Anusha, N. Sateesh, R. Subbiah, S. Vijayakumar, Multi-objective optimization using Taguchi based grey relational analysis in friction stir welding for dissimilar aluminium alloy, *International Journal on Interactive Design and Manufacturing* **18** (2024) 1627-1644. https://doi.org/10.1007/s12008-023-01529-9

[11] C. Chanakyan, S. Sivasankara, M. Meignanamoorthy, S. V. Alagarsamy, Parametric optimization of mechanical properties via FSW on AA5052 using Taguchi based grey relational analysis, *INCAS Bulletin* **13(2)** (2021) 21-30. https://doi.org/10.13111/2066-8201.2021.13.2.3

[12] M. P. Jenarthanan, R. Jeyapaul, Analysis and optimization of machinability behavior of CFRP composites using fuzzy logic, *Pigment & Resin Technology* **44(1)** (2021) 48-55. https://doi.org/10.1108/PRT-11-2013-0107

[13] M. A. Afabor, E. Emozino, I. D. Friday, O. O. David, A. S. Abella, Predictive modelling of TIG welding process parameters: A comparative study of Taguchi, Fuzzy Logic, and response surface methodology, *Nigerian Journal of Technology* **44(1)** (2025) 48-56. https://doi.org/10.4314/njt.v44i1.6